Eidgenössische Technische Hochschule Zürich

Ecole polytechnique fédérale de Zurich
Politecnico federale di Zurigo
Swiss Federal Institute of Technology Zurich

Entropy stable ENO scheme*

U.S. Fjordholm, S. Mishra and E. Tadmor†

Research Report No. 2011-05
February 2011

Seminar für Angewandte Mathematik
Eidgenössische Technische Hochschule
CH-8092 Zürich
Switzerland

*Partially supported by NSF grants DMS07-07949, DMS10-08397 and ONR grant N000140910385.

†Dept. of Mathematics, University of Maryland, MD 20742-4015, USA

Entropy stable ENO scheme*

Ulrik S. Fjordholm
Seminar for Applied Mathematics, ETH Zürich
HG J. 48, Rämistrasse 101, Zürich, Switzerland.
ulrikf@sam.math.ethz.ch

Siddhartha Mishra
Seminar for Applied Mathematics, ETH Zürich
HG G. 57.2, Rämistrasse 101, Zürich, Switzerland.
smishra@sam.math.ethz.ch

Eitan Tadmor
Center for Scientific Computation and Mathematical Modeling
and
Department of Mathematics, Institute for Physical Science & Technology
University of Maryland, College Park, MD 20742, USA
E-mail: tadmor@cscamm.umd.edu

Abstract

We prove the first stability estimates for the ENO reconstruction procedure. They take the form of a sign property: we show that the jump in the reconstructed pointvalues at each cell interface has the same sign as the jump in underlying cell averages (cell centered values) across the interface. Moreover their ratio is upper bounded. These estimates hold for arbitrary orders of accuracy of the reconstruction as well as for non-uniform meshes. We then combine the ENO reconstruction together with entropy conservative fluxes to construct new entropy stable ENO schemes of arbitrary order.

1 Introduction

The Essentially Non-Oscillatory (ENO) method was designed by Harten et al. in [8] for approximating solutions of nonlinear hyperbolic conservation laws. Let $\{x_{i+1/2}\}_{i\in\mathbb{Z}}$ be a given mesh, and define the cells $\mathcal{I}_i := [x_{i-1/2}, x_{i+1/2})$ and their sizes $h_i = x_{i+1/2} - x_{i-1/2}$ and $h = \max_i h_i$.

*Partially supported by NSF grants DMS07-07949, DMS10-08397 and ONR grant N000140910385.

The starting point is the collection $\{\overline{v}_i\}_{i\in\mathbb{Z}}$ of cell averages of a given function $v(x)$,

$$\overline{v}_i := \frac{1}{h_i}\int_{\mathcal{I}_i} v(x)dx, \tag{1.1}$$

from which we get the piecewise constant approximation

$$\mathcal{A}v(x) = \sum_{i\in\mathbb{Z}} \overline{v}_i \ \ 1_{\mathcal{I}_i}(x)$$

of v, which, when v is piecewise continuous, is accurate to first order. The role of the *ENO reconstruction method* is to construct a p-th ($p\in\mathbb{N}$) order accurate approximation

$$\mathcal{R}\mathcal{A}v(x) = \sum_{i\in\mathbb{Z}} f_i(x)1_{\mathcal{I}_i}(x)$$

of v, where $f_i\in\Pi_{p-1}$ is a polynomial recovered from neighboring cell averages. Each interpolant f_i is p-th order accurate in the sense that

$$f_i(x) = v(x) + \mathcal{O}(h^p) \qquad \text{for } x\in\mathcal{I}_i. \tag{**Accuracy**}$$

The function f_i is an interpolant in the sense that it preserves cell averages,

$$\frac{1}{h_i}\int_{\mathcal{I}_i} f_i(x)dx = \overline{v}_i, \tag{**Conservation**}$$

that is, $\mathcal{A}\mathcal{R}\mathcal{A} = \mathcal{A}$. To ensure the conservation property, we consider the primitive of v,

$$V(x) := \int_{-\infty}^{x} v(s)ds.$$

Letting $V_{j+1/2} = V(x_{j+1/2})$, it follows from (1.1) that

$$V_{j+1/2} := \int_{-\infty}^{x_{j+1/2}} v(s)ds = \sum_{i=-\infty}^{j}\int_{x_{i-1/2}}^{x_{i+1/2}} v(s)ds = \sum_{i=-\infty}^{j} h_i\overline{v}_i. \tag{1.2}$$

Therefore, given the cell averages $\{\overline{v}_i\}_i$, point values of the primitive V at the cell interfaces $x_{i+1/2}$ can be explicitly evaluated, up to an additive constant. Now, let $\mathbf{V}(x)$ be the unique p-th order polynomial interpolating the $p+1$ point values $V_{i-r-1/2},\dots,V_{i-r+p+1/2}$. We define the $(p-1)$-th order polynomial $f(x) = \mathbf{V}'(x)$. It is a simple consequence of (1.2) that f satisfies (**Accuracy**) and (**Conservation**). Hence, a *reconstruction* from cell averages requires an *interpolation* of the primitive.

Both the accuracy and conservation requirements can be met by interpolating the primitive V on any of the p stencils

$$\mathcal{S}_i^r = \{x_{i-r-1/2},\dots,x_{i-r+p+1/2}\},$$

where $r \in \{0, \dots, p-1\}$ is the *stencil offset*. As we are interested in approximating piecewise smooth functions, this stencil has to be selected carefully to avoid spurious oscillations in the reconstructed function. The principal idea of the ENO procedure is to choose the stencil offset in an iterative manner, based on divided differences. The ENO algorithm is defined as follows.

Algorithm 1.1 (ENO stencil selection procedure)**.** *Let point values of the primitive $V_{i-p-1/2}, \dots, V_{i+p+1/2}$ be given.*

- *Let $r_1 = 0$.*
- *For each $j = 1, \dots, p-1$: If*

  $$\left|V\left[x_{i-r_j-3/2}, \dots, x_{i-r_j+j-1/2}\right]\right| < \left|V\left[x_{i-r_j-1/2}, \dots, x_{i-r_j+j+1/2}\right]\right|$$

  then let $r_{j+1} = r_j + 1$; otherwise, let $r_{j+1} = r_j$.
- *Let $r = r_p$ and interpolate V over the stencil $\mathcal{S}_i^r$.*

As the j-th order divided difference of a function is a good measure of its j-th derivative, we obtain an interpolating polynomial with the smallest possible derivatives. Thus, the ENO procedure involves a *nonlinear data dependent* selection of the stencil in the *direction of smoothness* of the underlying piecewise smooth function.

Given the reconstructed function $\mathcal{RA}v = \sum_i f_i \ \mathcal{I}_i$, we obtain at each cell interface p-th order accurate approximations

$$v_i^- = f_i(x_{j-1/2}), \qquad v_i^+ = f_i(x_{i+1/2}) \tag{1.3}$$

such that

$$v_i^- = v(x_{i-1/2}) + \mathcal{O}(h^p), \qquad v_i^+ = v(x_{i+1/2}) + \mathcal{O}(h^p). \tag{1.4}$$

These values are the inputs to high-order accurate finite volume schemes to approximate nonlinear conservation laws (see Shu [17]), and the relation between these values and the cell averages will be the main point of study in this paper.

Despite of the existence of the ENO reconstruction procedure for the last 25 years, no global (mesh independent) stability results are available. Given this background, we present the following stability theorem.

Theorem 1.1. *[the sign property of ENO reconstruction [5]] Let $p \in \mathbb{N}$, and let v_i^+, v_{i+1}^- be left and right values at a cell interface $x_{i+1/2}$, obtained through a p-th order ENO reconstruction of cell averages $\{\overline{v}_i\}_i$. Then*

$$\operatorname{sgn}\left(v_{i+1}^- - v_i^+\right) = \operatorname{sgn}\left(\overline{v}_{i+1} - \overline{v}_i\right) \qquad (i \in \mathbb{Z}). \tag{1.5}$$

Moreover, there is a constant $\mathcal{C}_p$, depending only on p and on the ratios of neighboring grid cells, $\frac{h_{j+1}}{h_j}$, such that

$$0 \le \frac{v_{i+1}^- - v_i^+}{\overline{v}_{i+1} - \overline{v}_i} \le \mathcal{C}_p \qquad (i \in \mathbb{Z}). \tag{1.6}$$

The sign property says that at each cell interface, the jump in reconstructed values has the same sign as the jump in the underlying cell averages.

We remark that the above theorem is valid for any order of reconstruction and for any mesh size. It is valid for non-uniform meshes and makes no assumptions on the function v, other than that the cell averages $\overline{v}_i$ must be well-defined, which is guaranteed if e.g. $v \in L^1_{\text{loc}}(\mathbb{R})$.

The sign property is illustrated in Figure 1.1, where we show a third-, fourth- and fifth-order ENO reconstruction of randomly chosen cell averages. Even though the reconstructed polynomial can have large variations within a cell, its jumps at cell interfaces always have the same sign as the jumps of the cell averages.

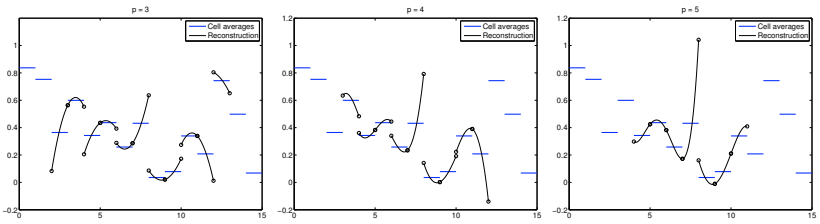

Figure 1.1: ENO reconstruction of randomly chosen cell averages.

The ENO procedure for reconstructing piecewise polynomials, given the point values of a piecewise smooth function $v_i = v(x_i)$ can be defined analogously, see [17]. This procedure is also stable in the following sense,

Theorem 1.2. *[5] Let $p \in \mathbb{N}$, and let v_i^+, v_{i+1}^- be left and right values at a cell interface $x_{i+1/2}$, obtained through a p-th order ENO reconstruction of point values $\{v_i\}_i$. Then*

$$\operatorname{sgn}\big(v_{i+1}^- - v_i^+\big) = \operatorname{sgn}\big(v_{i+1} - v_i\big) \qquad (i \in \mathbb{Z}). \tag{1.7}$$

Moreover, there is a constant $\widehat{\mathcal{C}}_p$, depending only on p and on the ratios of neighboring grid cells, $\frac{h_{j+1}}{h_j}$, such that

$$0 \leq \frac{v_{i+1}^- - v_i^+}{v_{i+1} - v_i} \leq \widehat{\mathcal{C}}_p \qquad (i \in \mathbb{Z}). \tag{1.8}$$

This sign property for the ENO reconstruction from point values will be used to construct arbitrarily high-order accurate *entropy stable* ENO schemes for systems of conservation laws in section 2 below.

Our stability results should be compared with that of existing *local* stability results for the ENO procedure like the stability result of [7] that for a given function v, there is an upper mesh size $h_0 > 0$ and a function $z(x)$, *both dependent on* v, such that

$$f(x) = z(x) + \mathcal{O}(h^p)$$

and

$$\mathrm{TV}(z) \leq \mathrm{TV}(v)$$

whenever the mesh size h is less than h_0. What is more, z is monotone inside cells where v has a discontinuity. For ENO-based finite volume or finite difference schemes, this result is of limited utility, as the approximate solution v depends on h.

There are some rigorous results about the global accuracy of the ENO procedure. In [1], the authors were able to show that the ENO method is globally second-order accurate when approximating a continuous function in one space dimension. This result should be contrasted with the global first-order accuracy of linear interpolation methods for continuous functions. Multi-dimensional global accuracy results were obtained in [2].

The ENO reconstruction procedure has been very successfully employed to approximate systems of hyperbolic conservation laws, [8, 15, 17]. Extensions of the ENO method like subcell resolution [9], ENO with biasing [16] and Weighted ENO (WENO) schemes [15, 17] have also been employed in computational fluid dynamics with considerable success. See the excellent review article [17] of Shu for an overview.

However, there are no rigorous stability proofs for any of the above ENO schemes. In the following, we will present a conservative finite difference scheme that approximates systems of conservation laws to arbitrarily high order of accuracy and is entropy stable.

2 Entropy stable ENO schemes

2.1 Continuous setting

In one space dimension, a system of conservation laws takes the form,

$$\begin{aligned} \mathbf{U}_t + \mathbf{f}(\mathbf{U})_x = 0, \quad \forall\ (x,t) \in \mathbb{R} \times \mathbb{R}_+, \\ \mathbf{U}(x,0) = \mathbf{U}_0(x), \quad \forall\ x \in \mathbb{R}. \end{aligned} \tag{2.1}$$

Here, $\mathbf{U} : \mathbb{R} \times \mathbb{R}_+ \mapsto \mathbb{R}^m$ is the vector of unknowns and $\mathbf{f}$ is the (nonlinear) flux vector.

It is well known ([3]) that solutions of (2.1) contain discontinuities in form of *shock waves*, even for smooth initial data. Hence, solutions of (2.1) are sought in a weak sense. Weak solutions may not be unique and need to be supplemented with extra admissibility criteria, termed as *entropy conditions*, in order to single out a physically relevant solution [3]. Assume that there exists a convex function $E : \mathbb{R}^m \mapsto \mathbb{R}$ and functions $\mathbf{V}, Q$ such that

$$\mathbf{V} = \partial_{\mathbf{U}} E, \quad \partial_{\mathbf{U}} Q = \langle \mathbf{V}, \partial_{\mathbf{U}} \mathbf{f} \rangle. \tag{2.2}$$

Then, a straightforward calculation using (2.1) and (2.2) shows that *smooth* solutions of (2.1) satisfy the *entropy identity*:

$$E_t + Q_x = 0. \tag{2.3}$$

However, the solutions of (2.1) are not smooth in general and the entropy has to be dissipated at shocks. Hence, we obtain an *entropy inequality*,

$$E_t + Q_x \leq 0, \tag{2.4}$$

that holds in the sense of distributions. We term Q and $\mathbf{V}$ in (2.2) as the entropy flux function and the vector of entropy variables, respectively. Integrating (2.4) over space results in the bound:

$$\frac{d}{dt}\int_{\mathbb{R}} E dx \leq 0 \quad \Rightarrow \quad \int_{\mathbb{R}} E\left(\mathbf{U}(x,T)\right) dx \leq \int_{\mathbb{R}} E(\mathbf{U}_0(x)) dx, \quad \forall T > 0. \tag{2.5}$$

As E is convex, the above entropy bound can be converted into an a priori estimate on the solution of (2.1) in suitable L^p spaces [3].

2.2 Conservative finite difference schemes

For simplicity, we consider a uniform Cartesian mesh $\{(x_i)\}$ in $\mathbb{R}$ with mesh size $x_{i+1} - x_i = \Delta x$. The midpoint values are $x_{i+1/2} = \frac{x_i + x_{i+1}}{2}$ and the domain is partitioned into intervals $I_i = [x_{i-1/2}, x_{i+1/2}]$. The conservative finite difference (finite volume) method updates point values (cell averages in I_i) of the solution $\mathbf{U}$ resulting in the semi-discrete scheme:

$$\frac{d}{dt}\mathbf{U}_i(t) = -\frac{1}{\Delta x}\left(\mathbf{F}_{i+1/2}(t) - \mathbf{F}_{i-1/2}(t)\right), \tag{2.6}$$

with numerical flux $\mathbf{F}_{i+1/2} = \mathbf{F}(\mathbf{U}_i(t), \mathbf{U}_{i+1}(t))$ computed from the (approximate) solution of the Riemann problem for (2.1) at the interface $x_{i+1/2}$, [13]. Second order spatial accuracy can be obtained with non-oscillatory TVD [11] and even higher order of accuracy can be obtained with ENO [8] and WENO [15] piecewise polynomial reconstructions.

However, these high-order schemes are not rigorously shown to be stable. As mentioned before, we will construct stable arbitrarily high-order conservative finite difference schemes. We do so in two stages.

2.3 Entropy conservative schemes

First, we construct entropy conservative schemes i.e, finite difference schemes of the form (2.6) which satisfy a discrete version of the entropy identity (2.3). Introducing the notation,

$$[\![a]\!]_{i+1/2} = a_{i+1} - a_i, \quad \overline{a}_{i+1/2} = \frac{1}{2}(a_i + a_{i+1}),$$

we follow the general procedure developed in [19] to define two-point entropy conservative fluxes:

Theorem 2.1. *(Tadmor, [19]:) Consider the one dimensional system of conservation laws (2.1) with entropy function E, entropy variables $\mathbf{V}$, entropy flux Q and define the entropy potential $\psi := \langle \mathbf{V}, \mathbf{f} \rangle - Q$. Let the finite difference scheme (2.6) approximate (2.1) and the numerical flux be given by $\mathbf{F}_{i+1/2} = F^*_{i+1/2} = \mathbf{F}^*(\mathbf{U}_i, \mathbf{U}_{i+1})$. We assume that it is consistent with $\mathbf{f}$ i.e $\mathbf{F}^*(\mathbf{U}, \mathbf{U}) = \mathbf{f}(\mathbf{U})$ and satisfies the following,*

$$\langle [\![\mathbf{V}]\!]_{i+1/2}, \mathbf{F}^*_{i+1/2} \rangle = [\![\psi]\!]_{i+1/2}, \quad \forall i. \tag{2.7}$$

Then the scheme (2.6) with numerical flux (2.7) satisfies the discrete entropy identity,

$$\begin{aligned} \frac{d}{dt}(E(\mathbf{U}_i)(t)) &= -\frac{1}{\Delta x}(\tilde{Q}_{i+1/2} - \tilde{Q}_{i-1/2}), \\ \tilde{Q}_{i+1/2} &= \left\langle \frac{(\mathbf{V}_i + \mathbf{V}_{i+1})}{2}, \mathbf{F}^*_{i+1/2} \right\rangle - \frac{(\psi_i + \psi_{i+1})}{2}. \end{aligned} \tag{2.8}$$

Summing over all i, we obtain entropy conservation:

$$\frac{d}{dt} \sum_i E_i \equiv 0.$$

Furthermore, the scheme (2.6) with flux $\mathbf{F}^*$ is second-order accurate.

We note that the condition (2.7) provides a single algebraic equation for m unknowns. In general, it is not clear whether a solution of (2.7) exists. Furthermore, the solutions of (2.7) will not be unique except in the case of scalar equations i.e, $m = 1$. In [19], Tadmor showed the existence of at least one solution of (2.7) for any system of conservation laws. Explicit solutions were constructed in [20]. However, the entropy conservative fluxes of [20] are computationally expensive, [4]. Instead, we follow recent papers [4, 14] to obtain algebraically simple and computational inexpensive solutions of (2.7). As an example, we consider the Euler equations of gas dynamics i.e, (2.1) with

$$\mathbf{U} = (\rho, \rho u, \mathcal{E})^\top, \quad \mathbf{f} = \left(\rho u, \rho u^2 + p, (\mathcal{E} + p)u\right)^\top \tag{2.9}$$

Here, ρ, u and p are the density, velocity and pressure of the fluid. The total energy $\mathcal{E}$ is related to other variables by the equation of state:

$$\mathcal{E} = \frac{p}{\gamma - 1} + \frac{1}{2}\rho u^2, \tag{2.10}$$

with γ being the gas constant. Let $s = \log(p) - \gamma \log(\rho)$ be the thermodynamic entropy. An entropy-entropy flux pair for the Euler equations is

$$E := \frac{-\rho s}{\gamma - 1}, \quad Q := \frac{-\rho u s}{\gamma - 1}. \tag{2.11}$$

The corresponding entropy variables and potential are

$$\mathbf{V} = \left\{ \frac{\gamma - s}{\gamma - 1} - \frac{\rho u^2}{2p}, \ \frac{\rho u}{p}, \ -\frac{\rho}{p} \right\}, \qquad \psi = \rho u. \tag{2.12}$$

An explicit entropy conservative flux for the Euler equations (see [14]) is given by

$$\begin{aligned} &\mathbf{F}^*_{i+1/2} = \{\mathbf{F}^{1,*}_{i+1/2}, \mathbf{F}^{2,*}_{i+1/2}, \mathbf{F}^{3,*}_{i+1/2}\}, \quad \mathbf{F}^{1,*}_{i+1/2} = \overline{z}_{2,i+1/2} (z_3)^{\ln}_{i+1/2}, \\ &\mathbf{F}^{2,*}_{i+1/2} = \frac{\overline{z}_{3,i+1/2}}{\overline{z}_{1,i+1/2}} + \frac{\overline{z}_{2,i+1/2}}{\overline{z}_{1,i+1/2}} \mathbf{F}^{1,*}_{i+1/2}, \quad \mathbf{F}^{3,*}_{i+1/2} = \frac{1}{2} \frac{\overline{z}_{2,i+1/2}}{\overline{z}_{1,i+1/2}} \left(\frac{\gamma+1}{\gamma-1} \frac{(z_3)^{\ln}_{i+1/2}}{(z_1)^{\ln}_{i+1/2}} + \mathbf{F}^{2,*}_{i+1/2} \right) \end{aligned} \tag{2.13}$$

Here, the parameter vectors are defined as

$$\mathbf{z} = (z_1, z_2, z_3) = \left\{ \sqrt{\frac{\rho}{p}}, \sqrt{\frac{\rho}{p}} u, \sqrt{\rho p} \right\}, \tag{2.14}$$

and $a^{\ln}$ is the logarithmic mean defined as

$$(a)^{\ln}_{i+1/2} := \frac{[\![a]\!]_{i+1/2}}{[\![\log(a)]\!]_{i+1/2}}. \tag{2.15}$$

Other examples of explicit two-point entropy conservative fluxes are described in [6].

2.3.1 High-order entropy conservative fluxes

We follow the procedure of LeFloch, Mercier and Rohde [12] in order to obtain arbitrary order accurate entropy conservative fluxes.

Theorem 2.2. *Consider the system (2.1), equipped with the entropy function E. Assume that there exists the two-point entropy conservative flux, $\mathbf{F}^*_{i+1/2} = \mathbf{F}^*(\mathbf{U}_i, \mathbf{U}_{i+1})$ satisfying (2.7). For any integer $p \geq 1$, define the numerical flux,*

$$\mathbf{F}^{2p,*}_{i+1/2} = \sum_{\{0 \leq r,s \leq p\}} \alpha_{rs} \mathbf{F}^*(\mathbf{U}_{i-r}, \mathbf{U}_{i+s}). \tag{2.16}$$

The co-efficients α_{rs} satisfy the consistency condition: $\sum_{r,s} \alpha_{rs} = 1$, and are computed using a Taylor expansion as in [12]. Then, the finite difference scheme (2.6) with numerical flux (2.16) satisfies the following properties:

(i.) The scheme is $2p$-th order accurate i.e, the truncation error of the scheme (2.6) satisfies,

$$\mathcal{T}_i(t) = \mathcal{O}(\Delta x^{2p}), \quad \forall, \quad \forall t > 0,$$

provided that the solutions of (2.1) are sufficiently smooth.

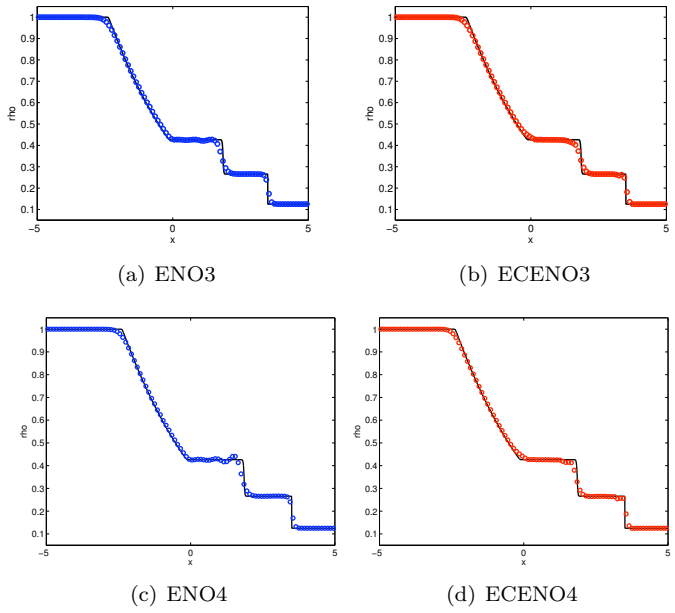

(a) ENO3 (b) ECENO3

(c) ENO4 (d) ECENO4

Figure 2.1: Comparing ENO (blue circles) and ECENO (red circles) with the reference solution (black line) for the Sod shock tube. Density at $T = 1.3$ on a mesh of 100 points is plotted.

(ii.) The scheme (2.6) with numerical flux (2.16) is entropy conservative as it satisfies the discrete entropy identity:

$$\begin{aligned} \frac{d}{dt}(E(\mathbf{U}_i)(t)) &= -\frac{1}{\Delta x}(\tilde{Q}^p_{i+1/2} - \tilde{Q}^p_{i-1/2}), \\ \tilde{Q}^p_{i+1/2} &= \frac{1}{2}\sum_{r,s} \alpha_{rs} \left(\langle (\mathbf{V}_{i-r} + \mathbf{V}_{i+s}), \mathbf{F}^*(\mathbf{U}_{i-r}, \mathbf{U}_{i+s}) \rangle - (\psi_{i-r} + \psi_{i+s}) \right). \end{aligned} \tag{2.17}$$

Some explicit examples of (2.16) are described in [6]. We remark that the arbitrarily high-order entropy conservative fluxes are linear combinations of the two point entropy conservative flux (2.7). Hence, computationally inexpensive forms of (2.7) like (2.13) are absolutely essential to design a computationally tractable high-order entropy conservative scheme.

2.4 ENO based numerical diffusion operators

Entropy is only conserved if the solutions (2.1) are smooth. However, the solutions of (2.1) develop discontinuities and entropy is *dissipated* at

shocks resulting in the entropy inequality (2.4). Hence, entropy conservative schemes described in the previous section will lead to high-frequency oscillations near shocks (see [4] for numerical examples). Consequently, we need to add some dissipative mechanism to ensure that entropy is dissipated near shocks. This is achieved by designing suitable entropy stable numerical diffusion operators.

The resulting scheme (2.6) will have the numerical flux,

$$\mathbf{F}^k_{i+1/2} = F^{2p,*}_{i+1/2} - \frac{1}{2}\mathbf{D}_{i+1/2}\langle \mathbf{V}\rangle_{i+1/2}. \tag{2.18}$$

Here, $k \geq 1$ and $p = k/2$ if k is even or $p = (k+1)/2$ if k is odd. The flux $\mathbf{F}^{2p,*}$ is the high order entropy conservative flux given by (2.16). The matrix $\mathbf{D}$ is any symmetric positive definite matrix. We perform a *suitable* reconstruction of the entropy variables $\mathbf{V}$ and obtain some piecewise polynomial function $\mathbf{V}_i(x)$ of degree $k-1$ for $x \in I_i$. Denoting

$$\mathbf{V}_i^- = \mathbf{V}_i(x_{i-1/2}), \quad \mathbf{V}_i^+ = \mathbf{V}_i(x_{i+1/2}), \quad \text{and} \quad \langle \mathbf{V}\rangle_{i+1/2} = \mathbf{V}_{i+1}^- - \mathbf{V}_i^+, \tag{2.19}$$

completes the description of the numerical flux (2.18). We need to modify the reconstruction procedure in order to ensure entropy stability. If $B = \mathrm{diag}(b_1, \ldots, b_n)$ is a diagonal matrix and $s \in \mathbb{R}$, then we write

$$B \leq s$$

provided $b_j \leq s$ for all j, and similarly for $B \geq s$.

We present sufficient conditions for the reconstruction to be entropy stable below.

Lemma 2.1. *Consider the one dimensional system (2.1) with entropy variables $\mathbf{V}$. Let $\{\widehat{r}^l_{i+1/2}\}_{l=1}^m$ be a basis of $\mathbb{R}^m$ for each i. Define the matrix*

$$\widehat{R}_{i+1/2} = \left[\widehat{r}^1_{i+1/2} | \widehat{r}^2_{i+1/2} | \cdots | \widehat{r}^m_{i+1/2}\right].$$

Let $\widehat{\Lambda}_{i+1/2}$ be any diagonal matrix with non-negative entries. Define the numerical diffusion matrix:

$$\widehat{\mathbf{D}}_{i+1/2} = \widehat{R}_{i+1/2}\widehat{\Lambda}_{i+1/2}\widehat{R}^{-1}_{i+1/2}. \tag{2.20}$$

Let $\mathbf{V}_i(x)$ be a polynomial reconstruction of the entropy variables in the cell I_i. Assume that for each i, there exists a diagonal matrix $B_{i+1/2} \geq 0$ such that the following holds:

$$\langle V\rangle_{i+1/2} = \widehat{R}_{i+1/2}B_{i+1/2}\widehat{R}^\top_{i+1/2}[\![\mathbf{V}]\!]_{i+1/2} \tag{2.21}$$

Then the numerical scheme (2.6) with numerical flux,

$$\mathbf{F}^k_{i+1/2} = F^{2p,*}_{i+1/2} - \frac{1}{2}\widehat{\mathbf{D}}_{i+1/2}\langle \mathbf{V}\rangle_{i+1/2}, \tag{2.22}$$

is entropy stable, i.e. it satisfies the entropy dissipation estimate:

$$\frac{d}{dt}E(\mathbf{U}_i) + \frac{1}{\Delta x}\left(\widehat{Q}_{i+1/2} - \widehat{Q}_{i-1/2}\right) \leq 0, \tag{2.23}$$

where the numerical entropy flux function $\widehat{Q}$ *is defined as*

$$\widehat{Q}_i = \widetilde{Q}^{2p}_{i+1/2} - \frac{1}{2}\left\langle \overline{\mathbf{V}}_{i+1/2}\widehat{\mathbf{D}}_{i+1/2}\langle \mathbf{V}\rangle_{i+1/2}\right\rangle.$$

Here, $\widetilde{Q}^{2p}$ *is defined by replacing* $\mathbf{D}$ *by* $\widehat{\mathbf{D}}$ *in* (2.17).

The proof of this lemma is presented in [6]. We need to find a reconstruction procedure which satisfies the crucial requirement that the matrix B in (2.21) is positive. Let $\mathbf{V}_i, \mathbf{V}_{i+1}, \mathbf{V}_i^+, \mathbf{V}_{i+1}^-$ be given. Define the *scaled entropy variables*,

$$\mathbf{W}_i^{\pm} = R^{\top}_{i\pm 1/2}\mathbf{V}_i, \quad \widetilde{\mathbf{W}}_i^{\pm} = R^{\top}_{i\pm 1/2}\mathbf{V}_i^{\pm}.$$

Dropping the $\pm$ superscript for notational convenience, the condition (2.21) reads as

$$\langle \widetilde{\mathbf{W}}\rangle_{i+1/2} = B_{i+1/2}\langle \mathbf{W}\rangle_{i+1/2}.$$

This is a component-wise condition; denoting the l-th component of $\mathbf{W}_i$ and $\widetilde{\mathbf{W}}_i$ by w_i^l and $\widetilde{w}_i^l$, respectively, the above condition is equivalent to

$$\operatorname{sgn}\langle \widetilde{w}^l\rangle_{i+1/2} = \operatorname{sgn}\langle w^l\rangle_{i+1/2}, \quad \forall i, l. \tag{2.24}$$

Note that the above condition amounts to the sign property in theorem 1.1. As the ENO reconstruction procedure satisfies the sign property, we can use it to define an entropy stable arbitrarily high order numerical diffusion operator. We obtain an arbitrarily high-order entropy stable scheme by using the ENO reconstruction procedure to reconstruct w^l for each l. The properties of the scheme are summarized below:

Theorem 2.3. *For any* $k \geq 1$, *let* $2p = k$ *(if* k *is even) or* $2p = k+1$ *(if* k *is odd). Define the entropy conservative flux* $\mathbf{F}^{2p,*}$ *by* (2.16). *Let* $\langle \mathbf{V}\rangle$ *in* (2.22) *be defined by the* k*-th order accurate ENO reconstruction procedure. Then the finite difference scheme* (2.6) *with numerical flux* (2.22) *satisfies the following properties,*

- *(i.) The scheme is* k*-th order accurate for smooth solutions of* (2.1).
- *(ii.) The scheme satisfies the discrete entropy inequality* (2.23). *Hence, it is entropy stable.*

We term the arbitrarily high-order accurate entropy stable schemes as *ECENO* schemes as they combine entropy conservative (EC) and ENO schemes.

Although any basis $\{r^l\}_{l=1}^m$ of $\mathbb{R}^m$ and any diagonal matrix $\widehat{\Lambda}$ will suffice for constructing an entropy stable scheme, we choose the following,

$$\widehat{R} = R.$$

Here, R is the matrix of eigenvectors of the flux Jacobian, $\mathbf{f}_\mathbf{U}$ and Λ is a positive diagonal matrix that depends on the eigenvalues of the flux Jacobian. Two examples of the matrix $\widehat{\Lambda}$ are

(i.) **Roe type diffusion operator:**

$$\widehat{\Lambda} = |\Lambda|. \tag{2.25}$$

Here, Λ denotes the matrix of eigenvalues of $\mathbf{f}_\mathbf{U}$.

(ii.) **Rusanov type diffusion operator:**

$$\widehat{\Lambda} = |\lambda^{\max}_{i+1/2}|\mathbf{ID}, \tag{2.26}$$

with $\lambda^{\max}$ denoting the largest eigenvalue of $\mathbf{f}_\mathbf{U}$.

3 Numerical experiments

We test the following schemes:

ENOk: k-th order accurate standard ENO scheme in the MUSCL formulation [8].

ECENOk: k-th order accurate entropy stable scheme (2.6) with numerical flux (2.22),

for $k = 3, 4$ and 5 on a suite of numerical experiments. The ENO-MUSCL and ECENO schemes are semi-discrete and are integrated in time with a standard Runge-Kutta method.

We consider the Euler equations i.e, (2.1) with (2.9). The entropy function and entropy variables are given in (2.11), (2.12). We define the ECENO scheme with entropy conservative flux given by (2.13) and diffusion matrix being of the Roe type (2.25). The eigenvalues and eigenvectors of the Jacobian are computed at the average of the left and right states. The ENO-MUSCL schemes use the standard Roe numerical flux.

3.0.1 Sod shock tube

The Sod shock tube experiment considers the Euler equations with Riemann initial data,

$$\mathbf{U}(x,0) = \begin{cases} \mathbf{U}_L & \text{if } x < 0 \\ \mathbf{U}_R & \text{otherwise,} \end{cases} \tag{3.1}$$

with

$$\begin{bmatrix}\rho_L\\ u_L\\ p_L\end{bmatrix} = \begin{bmatrix}1\\ 0\\ 1\end{bmatrix}, \qquad \begin{bmatrix}\rho_R\\ u_R\\ p_R\end{bmatrix} = \begin{bmatrix}0.125\\ 0\\ 0.1\end{bmatrix},$$

in the computational domain $[-5, 5]$. The initial discontinuity breaks into a left going rarefaction wave, a right going shock wave and a right going contact discontinuity. The computed density with the ENO3, ENO4, ECENO3 and ECENO4 schemes at time $T = 1.3$ on a mesh of 100 points is shown in figure 2.1. The results show that the ENO and ECENO schemes are quite good at resolving the waves. The ENO4 scheme is slightly oscillatory behind the contact whereas the ECENO3 and ECENO4 schemes resolve all the waves without any noticeable oscillations.

3.0.2 Shock-Entropy wave interaction

This numerical example was proposed by Shu and Osher in [15] and is a good test of a scheme's ability in resolving a complex solution with both strong and weak shocks and highly oscillatory but smooth waves. The Euler equations are considered in the computational domain $[-5, 5]$ with initial data,

$$\mathbf{U}(x,0) = \begin{cases}\mathbf{U}_L & \text{if } x < -4\\ \mathbf{U}_R & \text{otherwise,}\end{cases}$$

with

$$\begin{bmatrix}\rho_L\\ u_L\\ p_L\end{bmatrix} = \begin{bmatrix}3.857143\\ 2.629369\\ 10.33333\end{bmatrix}, \qquad \begin{bmatrix}\rho_R\\ u_R\\ p_R\end{bmatrix} = \begin{bmatrix}1+\varepsilon\sin(5x)\\ 0\\ 1\end{bmatrix}.$$

We compute up to $t = 1.8$ using a 3rd order Runge-Kutta integration method for the 3rd-order schemes, and a 4th order Runge-Kutta method for the 4th and 5th order schemes. The CFL number is set to 0.5. As a reference solution, we compute with the ENO3 scheme on a mesh of 1600 grid points. The approximate solutions are computed on a mesh of 200 grid points, corresponding to about 7 grid points for each period of the entropy waves. The solution computed by the ENO and ECENO schemes are displayed in Figure 3.1. There are very minor differences between the ENO and ECENO schemes of the same order. The test also illustrates that the higher order schemes perform better than a low order scheme.

4 Conclusion

We prove a global stability property for the ENO reconstruction procedure. This property termed as the *sign property* says that the jump

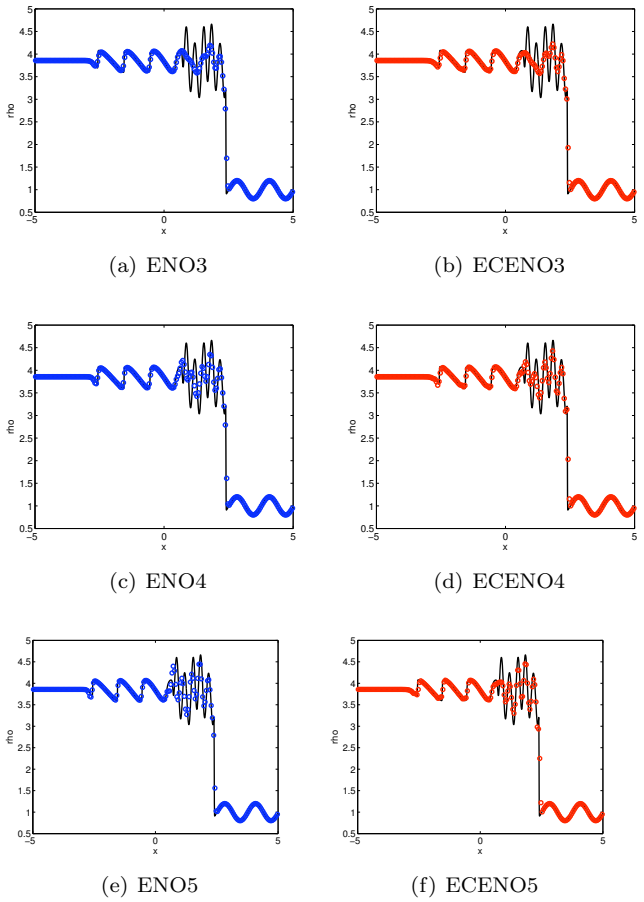

(a) ENO3 (b) ECENO3

(c) ENO4 (d) ECENO4

(e) ENO5 (f) ECENO5

Figure 3.1: Comparing ENO(blue circles) and ECENO (red circles) with a reference solution (black line) on the Shu-Osher shock-entropy wave interaction problem. The plotted quantity is the density at time $T = 1.8$ on a mesh of 200 points.

in the reconstructed values at each interface has the same sign as the jump in the underlying cell averages (cell centered values). We also obtain an upper bound of the jump in the reconstructed values in terms of the jump in the underlying values. The sign property is crucial in the construction of arbitrarily high-order accurate entropy stable schemes to approximate conservation laws. These schemes, termed as *ECENO* schemes are based on combining entropy conservative fluxes with suitable numerical diffusion operators. The numerical diffusion operators are constructed from a ENO reconstruction of scaled entropy variables. The resulting schemes are shown to be efficient in computations with the Euler equations. The paper presents results from recent articles [5, 6] that provide the first arbitrarily high-order finite difference schemes that are entropy stable for any system of conservation laws.

References

[1] F. Arandiga, A. Cohen, R. Donat and N. Dyn. Interpolation and approximation of piecewise smooth functions. *SIAM J. Num. Anal.,* 43 (1), 41-57, 2005.

[2] F. Arandiga, A. Cohen, R. Donat, N. Dyn and B. Matei. Approximation of piecewise smooth functions and images by edge-adapted (ENO-EA) nonlinear multiresolution techniques. *Appl. Comput. Har. Anal.,* 24, 225-250, 2008.

[3] C. Dafermos. *Hyperbolic conservation laws in continuum physics.* Springer, Berlin, 2000.

[4] U. S. Fjordholm, S. Mishra and E. Tadmor. Energy preserving and energy stable schemes for the shallow water equations. *"Foundations of Computational Mathematics"*, Proc. FoCM held in Hong Kong 2008 (F. Cucker, A. Pinkus and M. Todd, eds), London Math. Soc. Lecture Notes Ser. 363, pp. 93-139, 2009.

[5] U. S. Fjordholm, S. Mishra and E. Tadmor. ENO reconstruction is stable *preprint* 2010.

[6] U. S. Fjordholm, S. Mishra and E. Tadmor. Arbitrarily high-order accurate entropy stable essentially non-oscillatory schemes for systems of conservation laws. *In preparation,* 2010.

[7] A. Harten, B. Engquist, S. Osher and S. R. Chakravarty. Some results on high-order accurate essentially non-oscillatory schemes. *Appl. Num. Math.,* 2, 347-377, 1986.

[8] A. Harten, B. Engquist, S. Osher and S. R. Chakravarty. Uniformly high order accurate essentially non-oscillatory schemes. *J. Comput. Phys.*, 1987, 231-303.

[9] A. Harten. ENO schemes with subcell resolution. *J. Comput. Phys.,* 83, 148-184, 1989.

[10] G. Jiang and C-W. Shu. Efficient implementation of weighted ENO schemes. *J. Comput. Phys.,* 126, 1996. 202-226.

[11] B. VanLeer. Towards the ultimate conservative scheme V. A second-order sequel to Godunov's method. *J. Comput. Phys.,* 32, 1979, 101-136.

[12] P. G. LeFloch, J. M. Mercier and C. Rohde. Fully discrete entropy conservative schemes of arbitraty order. *SIAM J. Numer. Anal.,* 40 (5), 2002, 1968-1992.

[13] R. J. LeVeque. Finite volume methods for hyperbolic problems. *Cambridge university press,* Cambridge, 2002.

[14] P. L. Roe. Entropy conservative schemes for Euler equations. *Talk at HYP 2006, Lyon, France.* Unpublished, Lecture available from http://math.univ-lyon1.fr/ hyp2006.

[15] C. W. Shu and S. Osher. Efficient implementation of essentially non-oscillatory schemes - II, *J. Comput. Phys.*, 83, 1989, 32 - 78.

[16] C. W. Shu. Numerical experiments on the accuracy of ENO and modified ENO schemes. *J. Sci. Comput.,* 5 (2), 127-149.

[17] C. W. Shu. Essentially non-oscillatory and weighted essentially non-oscillatory schemes for hyperbolic conservation laws. *ICASE Technical report*, NASA, 1997.

[18] P. Sweby. High resolution schemes using flux limiters for hyperbolic conservation laws. *SIAM J. Num. Anal.*, 21, 1984, 995-1011.

[19] E. Tadmor. The numerical viscosity of entropy stable schemes for systems of conservation laws, I. *Math. Comp.,* 49, 91-103, 1987.

[20] E. Tadmor. Entropy stability theory for difference approximations of nonlinear conservation laws and related time-dependent problems. *Act. Numerica,* 451-512, 2004.

Research Reports

No.	Authors/Title
11-05	*U.S. Fjordholm, S. Mishra and E. Tadmor* Entropy stable ENO scheme
11-04	*M. Ganesh, S.C. Hawkins and R. Hiptmair* Convergence analysis with parameter estimates for a reduced basis acoustic scattering T-matrix method
11-03	*O. Reichmann* Optimal space-time adaptive wavelet methods for degenerate parabolic PDEs
11-02	*S. Mishra, Ch. Schwab and J. Šukys* Multi-level Monte Carlo finite volume methods for nonlinear systems of conservation laws in multi-dimensions
11-01	*V. Wheatley, R. Jeltsch and H. Kumar* Spectral performance of RKDG methods
10-49	*R. Jeltsch and H. Kumar* Three dimensional plasma arc simulation using resistive MHD
10-48	*M. Swärd and S. Mishra* Entropy stable schemes for initial-boundary-value conservation laws
10-47	*F.G. Fuchs, A.D. McMurry, S. Mishra and K. Waagan* Simulating waves in the upper solar atmosphere with Surya: A well-balanced high-order finite volume code
10-46	*P. Grohs* Ridgelet-type frame decompositions for Sobolev spaces related to linear transport
10-45	*P. Grohs* Tree approximation and optimal image coding with shearlets
10-44	*P. Grohs* Tree approximation with anisotropic decompositions
10-43	*J. Li, H. Liu, H. Sun and J. Zou* Reconstructing acoustic obstacles by planar and cylindrical waves
10-42	*E. Kokiopoulou, D. Kressner and Y. Saad* Linear dimension reduction for evolutionary data
10-41	*U.S. Fjordholm* Energy conservative and -stable schemes for the two-layer shallow water equations